

X-ray standing waves in garnet crystals

S. Lagomarsino, F. Scarinci, and A. Tucciarone

Istituto di Elettronica dello Stato Solido del Consiglio Nazionale delle Ricerche, Via Cineto Romano 42, 00156 Roma, Italy

(Received 3 January 1984)

Measurement of fluorescent radiation produced by x-ray standing waves is applied to site-occupancy determination in both thin layers and bulk garnet single crystals. The fluorescence yield for atoms in different crystallographic sites has been calculated for the (521) and (444) reflections in the case of gadolinium gallium garnet for both a thin layer and a bulk crystal. Primary extinction is discussed. We find that, although it may play a major role in determining the line shape of the fluorescence yield, the effect is not as dramatic in garnets as it is in silicon or germanium, so that different crystallographic sites give clearly distinctive fluorescence patterns even for bulk crystals. Finally, theoretical and experimental line shapes are compared.

I. INTRODUCTION

When an x-ray beam is diffracted by a perfect crystal, interference phenomena between the wave fields excited in the crystal give rise to a resulting wave field whose intensity has the functional form of a standing-wave pattern, as is well established by the dynamical theory of x-ray diffraction.¹ In the case of reflection, the standing-wave pattern is the same for each polarization state. The equi-intensity planes are parallel to and have the same periodicity of the diffracting planes (hkl). The standing-wave pattern has strong minima and maxima (and in certain cases nodes and antinodes), whose positions with respect to the crystal atoms change as a function of the angle between the incident beam and the crystal. In this way a modulation occurs in the interaction between the electromagnetic radiation and the crystal atoms. This modulation can be monitored by secondary events such as fluorescent emission,^{2,3} Compton and thermal x-ray scattering,⁴ and photoelectron yield.⁵

The modulation has been utilized to determine the interstitial or substitutional nature of impurity atoms.⁶ High-resolution measurements on this subject were first reported by Golovchenko *et al.*⁷ who observed the fluorescent emission of As atoms diffused in a Si (220) crystal. The As atoms were distributed in a surface layer 0.4 μm thick. Because of this, the modulation of the fluorescence yield was not influenced by the primary extinction (we will return to this subject later). In a subsequent work on the same system, but with the As atoms implanted rather than diffused and with improved experimental conditions, Andersen *et al.*⁸ achieved a spatial resolution of 0.02 \AA in the lattice location of As atoms. The technique has also been extended to surface-location studies,⁹ leading to the solution of the registration problem in the case of bromine atoms in submonolayer coverages on a Si(111) surface.¹⁰

To our knowledge, the technique has until now been applied only to crystals with quite simple structures, such as those with cubic-diamond (Si,Ge), or zinc blende (GaAs,GaP).¹¹⁻¹³ Furthermore, in the experiments re-

ferred to above,^{7-10,12,13} the excited atoms were in surface layers. In the materials investigated, the standing-wave method for atom localization within the structure loses resolution dramatically when extended to bulk measurements, because of extinction.

In this paper we report the application of x-ray standing-wave experiments to site-occupancy determination in bulk crystals and in thin films having the garnet structure.

II. APPLICATION TO GARNETS

The garnet structure, as is well known,¹⁴ belongs to the space group $Ia\bar{3}d$ with all the cations in special positions, with no positional degrees of freedom, and the oxygen atoms in the general positions. In the unit cell there are eight formula units of the type $\{A_3\}[B_2](C_3)O_{12}$, where the different sets of brackets represent sites with different coordination to oxygen, namely $\{ \}$ represents dodecahedral (c) sites, $[\]$ represents octahedral (a) sites, and $(\)$ represents tetrahedral (d) sites. A large variety of ions can occupy different sites, completely or partially, and many of the ions occupy more than one site. The site occupancy of substitutional ions can be determined by size considerations (the sites have different dimensions), and, for magnetic garnets, can be determined by magnetic measurements.¹⁵ The scope of this paper is to show that x-ray fluorescence under diffraction conditions has, for certain (hkl) reflections, markedly different dependences on the rocking angle for the different sites. This provides a *direct way* of determining cation site occupancy also in the case of low-substitutional levels, both in bulk crystals and epitaxial films. The technique can also be applied to nonmagnetic garnets. As a demonstration, the fluorescence yield has been calculated for different reflections and for the atoms of a $\text{Gd}_3\text{Ga}_5\text{O}_{12}$ (GGG) single crystal (Mo $K\alpha$ incident radiation).

The calculation has been carried out by considering that the fluorescence yield is proportional to the intensity I of the resulting wave field in the crystal at the atom location. I is given by the following relation:

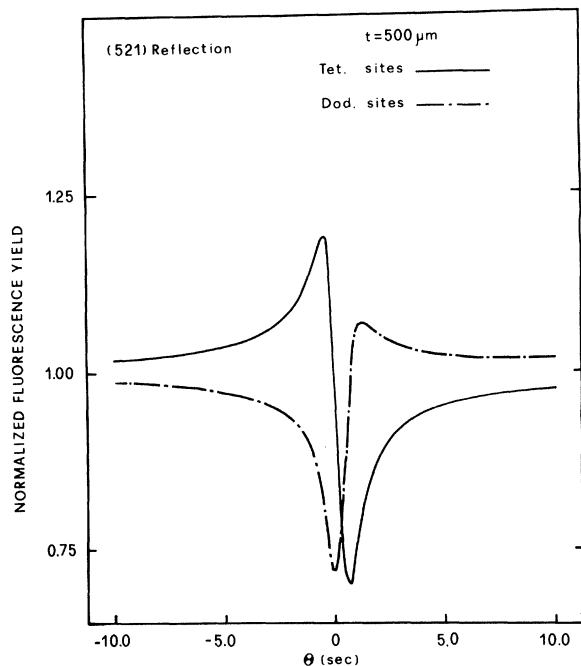


FIG. 1. Theoretical $Ga K\alpha$ and $Gd L\alpha$ fluorescence-yield curves for the GGG (521) reflection. $Mo K\alpha$ is the incident radiation. The result for Ga atoms in tetrahedral sites (—) and for Gd atoms in dodecahedral sites (-·-·-·) are shown. Thickness $t = 500 \mu m$.

$$I = I_0 \exp(-4\pi \vec{K}_0'' \cdot \vec{r}) \left| 1 + \left(\frac{E_H}{E_0} \right) \exp(2\pi i \vec{H} \cdot \vec{r}) \right|^2, \quad (1)$$

where I_0 is the incident intensity, \vec{H} is the reciprocal-lattice vector of the reflecting planes, \vec{r} is a position vector in the unit cell of the crystal, \vec{K}_0'' the imaginary part

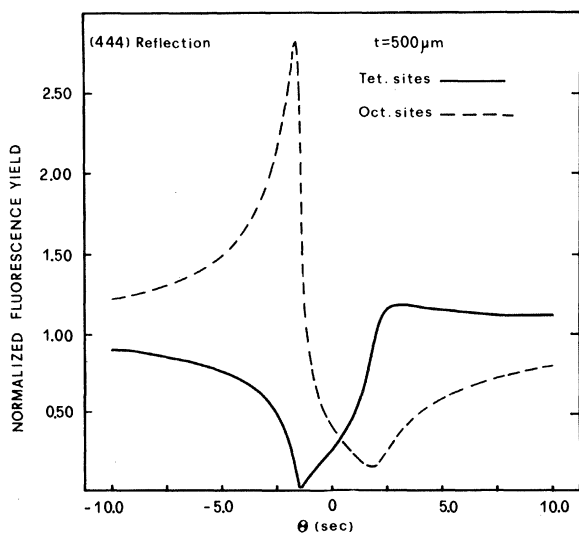


FIG. 2. Theoretical $Ga K\alpha$ fluorescence-yield curve for the GGG (444) reflection. $Mo K\alpha$ is the incident radiation. The result for Ga atoms in tetrahedral (—) and in octahedral (- - -) sites are shown. Thickness $t = 500 \mu m$.

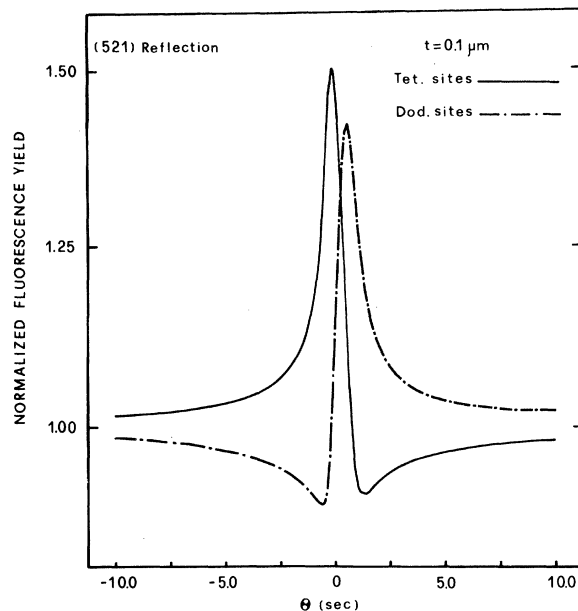


FIG. 3. Theoretical $Ga K\alpha$ and $Gd L\alpha$ fluorescence-yield curves for the GGG (521) reflection. $Mo K\alpha$ is the incident radiation. The result for Ga atoms in tetrahedral sites (—) and for Gd atoms in dodecahedral sites (-·-·-·) are shown. Thickness $t = 0.1 \mu m$.

of the inside "incident" wave vector (\vec{K}_0'' is always directed along the surface normal), and (E_H/E_0) is the ratio of the "incident" and "diffracted" field amplitudes inside the crystal.

Equation (1) has been calculated for all of the positions in the unit cell occupied by the atoms which give rise to a given fluorescence radiation, and the contributions from each position added together. Finally, contributions from the whole crystal thickness have been integrated, also taking into account the absorption of the fluorescence radiation by the crystal matrix (the GGG has very nearly the same absorption coefficient for the $Ga K\alpha$ and the $Gd L\alpha$ radiations). The calculation has been carried out for angular positions corresponding to the diffraction curve of a given reflection and normalized to unity for angular positions far from the Bragg condition. Figure 1 shows the result of such a calculation for the (521) reflection and for a crystal thickness of $500 \mu m$. The solid curve represents the fluorescence-yield modulation for atoms occupying tetrahedral sites, while the dotted-dashed curve refers to dodecahedral sites. The yield curve for octahedral sites has nearly the same behavior of the curve for tetrahedral sites. Figure 2 refers to the (444) reflection and to a crystal thickness of $500 \mu m$. In this case, the fluorescence-yield curves for octahedral sites (dashed curve) and for tetrahedral sites (solid curve) have markedly different behavior. The yield curve for dodecahedral sites is, in this case, exactly the same as the curve for tetrahedral sites.

As mentioned above, the modulation of the fluorescence yield due to diffraction is strongly affected by primary extinction: i.e., by the fact that, when diffraction takes place, the effective absorption coefficient of the incident beam is a strong function of the incidence angle

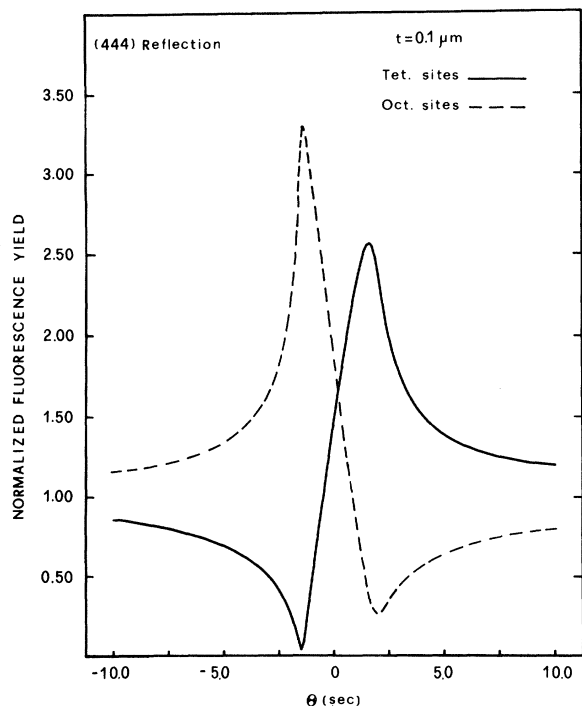


FIG. 4. Theoretical Ga $K\alpha$ fluorescence-yield curve for the GGG (444) reflection. Mo $K\alpha$ is the incident radiation. The result for Ga atoms in tetrahedral (—) and in octahedral (---) sites are shown. Thickness $t=0.1 \mu\text{m}$.

and has its maximum at the center of the diffraction curve, where it achieves several times the value due to photoelectron absorption.¹ Of course, the incident intensity is depleted in favor of the diffracted intensity, and this may play a major role in determining the line shape of the fluorescence yield. However, in garnets the effect is not as dramatic as in Si or Ge, and the distinction between the different crystallographic sites is still very clear, *even in a bulk crystal*, as shown in Figs. 1 and 2. For comparison, Figs. 3 and 4 show the fluorescence-yield modulation of the different sites for the (521) and (444) reflections, respectively, in the case of a relatively thin layer of 1000 Å. Comparison of the corresponding curves in Figs. 1 and 2 shows that the effect of primary extinction is strong, but does not mask the peculiar feature of the fluorescence-yield modulation. From this point of view, the situation in crystals with garnet structure (such as GGG) is quite favorable with respect to Si or Ge crystals. For example, the ratio between the penetration depth due to photoelectron absorption and the penetration depth due to primary extinction is 2 times greater for a Ge (220) reflection than it is for a GGG (444) reflection in the case of an incident Mo $K\alpha$ radiation.

If we also consider the absorption of the fluorescence radiation, we calculate that, in the case of Ga $K\alpha$ or Gd $L\alpha$ radiation in the (444) reflection of a GGG crystal (Mo $K\alpha$ incident radiation), the depth from which the measured fluorescence radiation is originated is, far from the Bragg condition, nearly 5 times the corresponding depth at the center of the diffraction curve. Instead, in

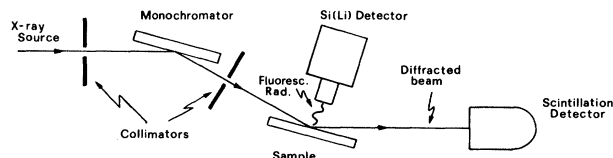


FIG. 5. Experimental geometry.

the case of the Ge (220) reflection (Mo $K\alpha$ incident radiation), the depth from which the measured Ge $K\alpha$ radiation is originated is, far from the Bragg condition, nearly 14 times the corresponding depth at the center of the diffraction curve. Evidently, it is possible to reduce or even to eliminate the effect due to primary extinction by a suitable geometry, but in any case with considerable loss of intensity (Ref. 12). To compare theoretical predictions with experimental data, x-ray fluorescence yield from GGG crystals has been measured.

III. EXPERIMENT

The $\{\text{Gd}_3\}[\text{Ga}_2](\text{Ga}_3)\text{O}_{12}$ crystals were commercially available as standard (111) substrates for epitaxial growth. The crystalline perfection of this kind of crystals, grown by the Czochralski technique, is very good with regard to dislocations and inclusions. In practice, crystals that are free of dislocations and inclusions can be obtained.¹⁶ However, growth striations are always present, due to compositional fluctuations; these cause lattice-parameter variations of the order of 0.0002 Å.¹⁷ The measurements were carried out on a double-crystal diffractometer, with the arrangement described in Fig. 5. The x-ray beam, Mo $K\alpha$ radiation from a conventional 0.8 kW fine-focus source, was diffracted by the monochromator, a high-perfection (111) orientation GGG crystal. The emergent

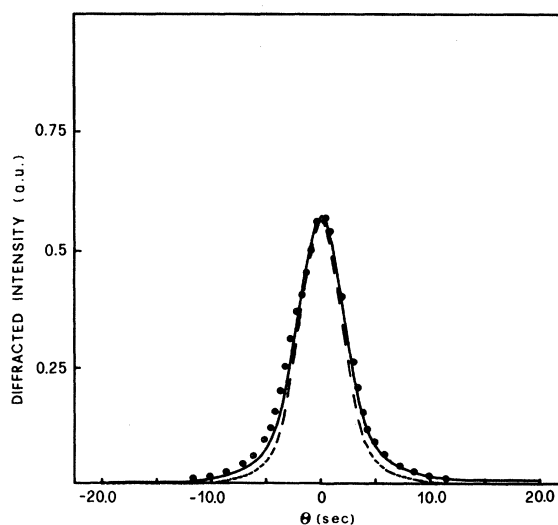


FIG. 6. GGG (444) diffraction curve with Mo $K\alpha$ incident radiation. Closed points are experimental data. Dashed curve is the theoretical Darwin-Prins curve convoluted with the reflectivity curve of the monochromator. The solid curve is the convolution of the dashed curve with a Lorentzian function to take into account the broadening due to structural defects (see text).

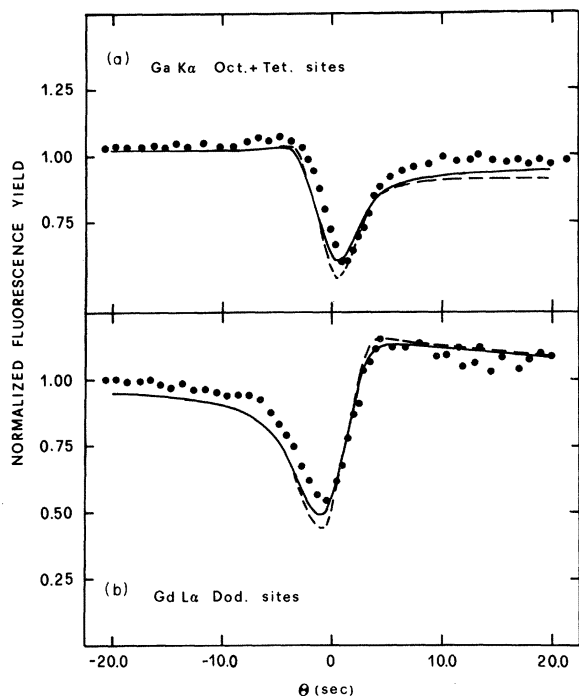


FIG. 7. X-ray fluorescence-yield curves of (a) Ga $K\alpha$ and (b) Gd $L\alpha$ radiations for GGG (444) reflection. Mo $K\alpha$ is the incident radiation. Closed points are experimental data. The dashed curve is the theoretical prediction for Ga atoms in octahedral and tetrahedral sites and for Gd atoms in dodecahedral sites. The solid curve is the convolution of the dashed curve with the same Lorentzian function used to take into account the broadening of the diffraction curve (see text and Fig. 6).

beam was then directed onto the sample and diffracted by it. In all cases, the same reflection was utilized for the sample and the monochromator. The measurements were carried out by rocking the sample step by step, while measuring, at each step, the second diffracted beam by a scintillation counter and by analyzing the x-ray fluorescence from the sample by a gas-cooled Si(Li) detector (Laben model no. MP 38) and a multichannel analyzer. The Gd $L\alpha$ and Ga $K\alpha$ radiations were detected.

IV. RESULTS AND DISCUSSION

Figure 6 presents the (444) diffraction curve of a GGG crystal. Closed points are experimental data. The dashed curve is the well-known Darwin-Prins curve,^{1,2} calculated by taking into account the absorption and convoluted with itself to account for the angular width from the reflectivity curve of the monochromator. The vertical scale is normalized to the experimental data. The full width at half maximum (FWHM) of the experimental diffraction curve is slightly (10%) larger than the theoretical curve. This is due to the presence of structural defects, probably caused by growth striations, as discussed earlier (see Sec. III). To account for this broadening, a phenomenological approach has been utilized. The theoretical curve was convoluted with a Lorentzian curve whose FWHM was the difference between the FWHM of the experimental and theoretical curves. The solid curve in Fig. 6 represents the

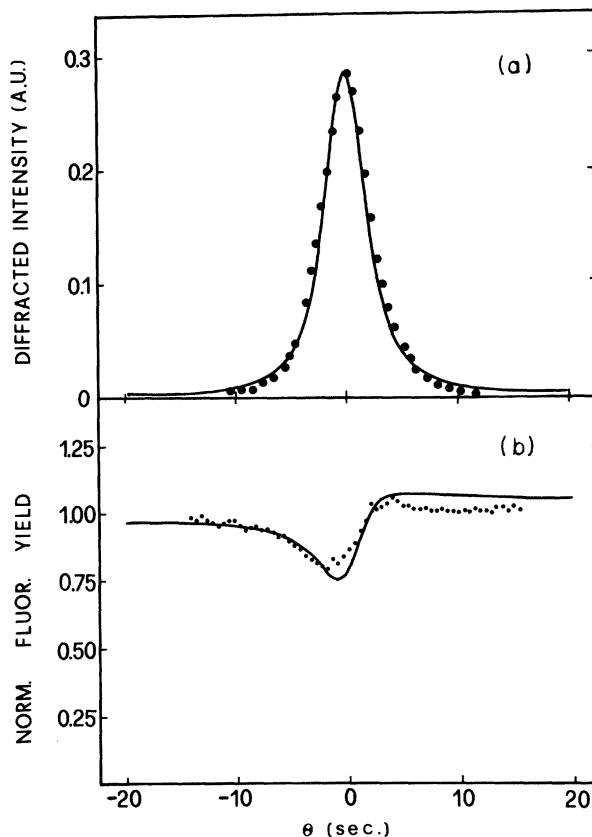


FIG. 8. (a) Diffraction curve and (b) fluorescence-yield curve of Ga $K\alpha$ radiation for GGG (888) reflection. Mo $K\alpha$ is the incident radiation. Closed points are experimental data. The solid curves are, as in Figs. 6 and 7, the result of a convolution between the theoretical curves and a function which accounts for the structural defects. The theoretical fluorescence yield has been calculated for Ga atoms in octahedral and tetrahedral sites. Gd atoms in dodecahedral sites give the same result.

result of this convolution. The matching with the experimental data is quite good. Figure 7 presents the x-ray fluorescence yield for (a) the Ga $K\alpha$ and (b) Gd $L\alpha$ radiations as the crystal is rotated through the diffraction curve shown in Fig. 6. Closed points are experimental data. The fluorescence yield is normalized to unity far from the Bragg condition. The horizontal origin is the center of the experimental diffraction curve. The theoretical fluorescence yield has been calculated according to the procedure described in Sec. II. In addition, the resulting curves have been convoluted with the reflectivity curve of the monochromator. In Fig. 7 the variation of the fluorescence yield with the angular position obtained by this procedure (dashed curve) refers to (a) Ga $K\alpha$ radiation for atomic location corresponding to octahedral and tetrahedral sites, and (b) Gd $L\alpha$ radiation for atomic location corresponding to dodecahedral sites. The solid curve is the convolution of the theoretical fluorescence yield with the same Lorentzian curve utilized to account for the discrepancy between the theoretical and experimental diffraction curves (see Fig. 6 and relative discussion). The matching with the experimental data is quite satisfactory. Finally, Fig. 8(a) shows the diffraction curve of the (888) reflection. Closed points are experimental data, and the

solid curve is the theoretical diffraction curve also obtained by taking into account the broadening due to defects. Figure 8(b) shows the corresponding modulation of the fluorescence yield of Ga $K\alpha$ radiation coming from atoms in octahedral and tetrahedral sites. The theoretical predictions (solid curve), obtained following the procedure described above for the (444) reflection, is in good agreement with the experimental data. For the (888) reflection all of the crystallographic sites give the same modulation. Effectively, the Gd $L\alpha$ fluorescence yield, not shown here, which comes from atoms in dodecahedral sites, has the

same dependence on the rocking angle as the Ga $K\alpha$ yield, both theoretically and experimentally.

In conclusion, it has been demonstrated that x-ray standing-wave experiments are possible in crystals having the garnet structure such as the GGG crystals, even in bulk crystals. For given reflections, the modulation of the fluorescence yield is different for different crystallographic sites. This can lead to a *direct* method of determining the site occupancy, also in case of low substitutional levels. Further work in this field is in progress, both for bulk crystals and for epitaxial films.

¹R. W. James, *The Optical Principles of the Diffraction of X-Rays* (Bell, London, 1954), Chap. VIII.

²B. W. Batterman and H. Cole, *Rev. Mod. Phys.* **36**, 681 (1964).

³B. W. Batterman, *Phys. Rev.* **133**, A759 (1964).

⁴S. Annaka, S. Kikuta, and K. Kohra, *J. Phys. Soc. Jpn.* **21**, 1559 (1966); S. Annaka, *ibid.* **24**, 1332 (1968).

⁵V. N. Shchemelev and M. V. Kruglov *Fiz. Tverd. Tela* (Leningrad) **14**, 3556 (1973) [*Sov. Phys.—Solid State* **14**, 2988 (1973)].

⁶B. W. Batterman, *Phys. Rev. Lett.* **22**, 703 (1969).

⁷J. A. Golovchenko, B. W. Batterman, and W. L. Brown, *Phys. Rev. B* **10**, 4239 (1974).

⁸S. K. Andersen, J. A. Golovchenko, and G. Mair, *Phys. Rev. Lett.* **37**, 1141 (1976).

⁹P. L. Cowan, J. A. Golovchenko, and M. F. Robbins, *Phys.*

Rev. Lett. **44**, 1680 (1980).

¹⁰J. A. Golovchenko, J. R. Patel, D. R. Kaplan, P. L. Cowan, and M. J. Bedzyk, *Phys. Rev. Lett.* **49**, 560 (1982).

¹¹P. Trucano, *Phys. Rev. B* **13**, 2524 (1976).

¹²T. Takahashi and S. Kikuta, *J. Phys. Soc. Jpn.* **47**, 620 (1979).

¹³J. R. Patel and J. A. Golovchenko, *Phys. Rev. Lett.* **50**, 1858 (1983).

¹⁴S. Geller and M. A. Gilleo, *J. Phys. Chem. Solids* **3**, 30 (1957).

¹⁵See, for example, *Physics of Magnetic Garnets, Proceedings of the International School of Physics, "Enrico Fermi," Course LXX*, edited by A. Paoletti (North-Holland, Amsterdam, 1977).

¹⁶C. D. Brandle, D. C. Miller, and J. W. Nielsen, *J. Cryst. Growth* **12**, 195 (1972).

¹⁷R. F. Belt and J. P. Moss, *Mater. Res. Bull.* **8**, 1197 (1973).